

Optimisation of Important Factors Influencing Spring-back after Sheet Metal Forming

Abdulaziz Alghtani

*Assistant Professor, Mechanical Engineering Department,
Taif University, Main campus,
Airport Road, Al Hawiyah Area 888. Taif 21974 ., Saudi Arabia.*

P.C. Brooks

*Assistant Professor, School of Mechanical Engineering,
University of Leeds,
Leeds LS2 9JT, UK*

D.C. Barton

*Professor, School of Mechanical Engineering,
University of Leeds,
Leeds LS2 9JT, UK*

V.V. Toropov

*Professor, School of Engineering and Materials Science
Queen Mary University,
Mile End Road, London E1 4NS, UK*

Abstract

Fabricating parts such as structural members of automobiles are achieved by using sheet metal forming technique. Light weight high strength materials are preferable to minimise the fuel consumption and therefore reducing the emissions. However, fabricating such materials are usually associated with some defects. One of the most announced phenomenon is called Spring-back; the deviation in specimen geometry subsequent to forming due to elastic recovery. The aim of the current research is to assess the effect of main forming process parameters on the Spring-back level. The U-drawing process was studied in this work, since this process supports more complex sheet metal forming operations. A reliable test rig for such operation was created and 3D finite element model was developed to simulate the process. The simulations for four different material were validated. An acceptable agreement between the simulations and experiments results were obtained, however, the high strength galvanised steel shows disagreement results. Parametric study was conducted to evaluate the influence of several parameters on the Spring-back magnitude. Finally, an optimisation method was developed to find the optimum parameters combination to reduce Spring-back level and successfully utilised to optimise the process parameters for the different materials studied.

Keywords: Spring-back, U-drawing process, design of experiment, optimisation, blank thickness, die radius, punch radius

INTRODUCTION

There is substantial concern about fuel consumption and

therefore CO₂ emissions arising from automobiles. Therefore, reducing the weight of vehicles could eliminate such issue by utilising light weight materials of high strength and improve performance, handling and comfort [1]. The old method of forming sheet metals was depend on the manufacturer experience and trial and error method which is costly and time consuming [2], therefore there is a need to improve this process in more systematic and scientific way.

Using high strength materials in sheet metal forming processes usually bring several defects. One of the most common faults is that associated with Spring-back of the used material. It is distinguished when the forming tool is released from the formed specimen, the specimen try to return to its originality. The problem of Spring-back is more found for the new high strength materials than for materials of low strength.

In the past many scientists have studied the elastic-plastic behaviour of materials and have developed appropriate material models, but usually within small distortion. However, sheet metal forming undertake large deformation subsequent to Spring-back phenomena because of the elastic recover [3]. The accurate simulation of Spring-back depends on a robust material model that describes the sheet material behaviour as it experiences large distortion bending and unbending that are typical of many forming processes [4].

Researchers have investigated experimentally the reverse yielding after plastic deformation for polycrystalline aluminium and related this to the dislocation structures developed in the material [5]. Scholars have investigated the stress reversals influence on the behaviour of work hardening of copper alloys [6]. Specialists studied the reverse yielding after plastic deformation for spheroidal steels recognising that the Bauschinger effect (early re-yielding during reverse deformation) should be utilized [7]. Yoshida and Uemori [8] succeeded in deriving an appropriate material model from the

results of a sequence of cyclic tension-compression large distortion experiments on steel and aluminium samples. Subsequently, the well-known Yoshida-Uemori model for large strain cyclic plasticity was achieved which was utilised for the present study [8].

The main purpose of the current study is to evaluate the ability of an advanced CAE method to simulate Spring-back after sheet metal forming processes and to improve an optimisation technique that can control the springback to reasonable magnitude. This paper identifies the blank materials used in the experiments and the main U-bending experiments and results. Then, the advanced CAD technique was conducted to develop 3D finite element model that can simulate such process and draw out the predicted Spring-back results compared with experiment. After that, a parametric study was utilised conducting the validated 3D model to examine the effect of physical parameters, such as die and punch radii, on spring-back. Finally an optimisation method was developed to reduce Spring-back level after the U-drawing sheet metal forming process, and good results were achieved.

MATERIALS AND U-DRAWING EXPERIMENTS

The current study uses a metal forming press previously made by the same author [9] as shown in Figure 1. Four different blank materials listed in Table 1 provided by Jaguar Land Rover Ltd ,UK, were laser cut into rectangular strips of 300 x 30 mm. Experiments conducted using Instron test machine as shown in Figure 1 which was explained in great details in [9] where, the punch speed and travel distance were 2 mm/s and 48 mm respectively as listed in Table 1. Then, the deformed part was released carefully after the forming process. A CMM machine was utilised to measure the deformed part as illustrated in Figure 2 (a). The straight lines AB, CD and EF were plotted through these points. Then, the θ_1 Spring-back angle is defined as the angle between line AB and line CD, and the angle θ_2 is confined between lines CD and EF. Figure 2 (b) shows that the Spring-back is more pronounced in high strength steel than the rest materials.

Table 1. Blank materials and experiments conditions

| Materials | Thickness (mm) | Punch speed (mm/s) | Punch travel distance (mm) |
|------------|----------------|--------------------|----------------------------|
| DP600 | 1.6 | 2 | 48 |
| DX54D | 1.6 | | |
| CPLA100K38 | 2.5 | | |
| CPLA10414 | 2.5 | | |

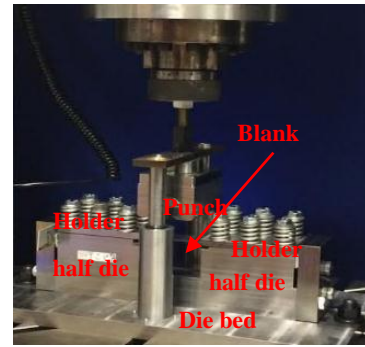


Figure 1: U-drawing rig mounted on Instron test machine

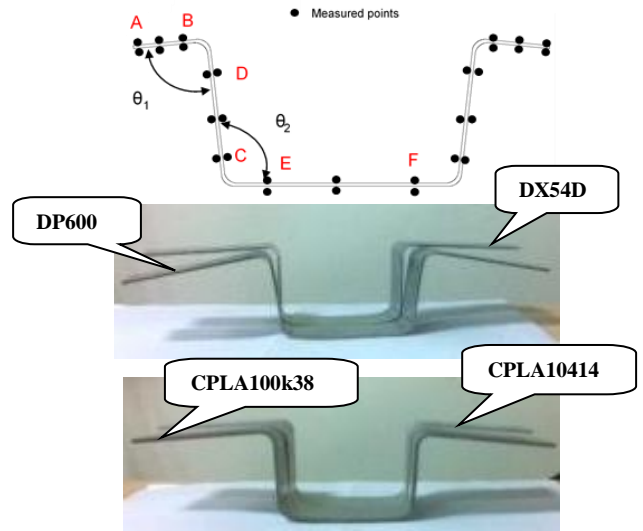


Figure 2: (a) Specimens showing Spring-back after the U-drawing process (b) measurement of Spring-back angles after the U-drawing process, showing approximate location of measurement points

The U-bending process was simulated based on 3-D quadratic shell elements based on the Reissner-Mindlin kinematic assumption [10] as shown in Figure 3 where the stress is assumed to be negligible through-thickness however it considers the shear deformations in the thin shell elements [11]. The Ls-Dyna software was utilised as a solver for the forming analysis using the explicit solution and the implicit solution algorithm for the prediction of Spring-back as recommended by many researchers. The first user for this approach were Lee and Yang (Lee and Yang, 1998) [12] where they use the explicit method for sheet metal forming analysis whilst Narasimhan and Lovell coupled this with an implicit solution for Spring-back prediction [13]. Furthermore, Behrouzi et al., have proved the efficacy of this coupled implicit-explicit algorithm technique for the Spring-back prediction [14].

The applied boundary conditions were as specified in Figure 3 where, the punch, die and blank holder were assigned as rigid parts, while the blank was assigned as a deformable part. A contact between the punch, die, blank and blank holder components was determined by one way surface-to-surface regime. In this kind of contact, a master surface was assigned for the rigid bodies, however the deformable body was defined as a slave surface. As a part of contact conditions friction coefficients should be defined between the interfaces,

therefore static and dynamic friction coefficients for all four materials sliding against tools surfaces were measured by the current author as listed in Table 3. Table 2 illustrates the geometry parameters of the U-bending model. The steps of developed numerical U-drawing process model conducted in the current study was as illustrated in Figure 4. The parameters of the Y-U material model for the blank materials used in the current study were listed in Table 3.

Table 2: Baseline dimensions of the U-bending model

| | | Dimension (mm) | Material |
|------------------------|---|----------------|----------|
| Geometrical Parameters | L | 150 | |
| | D | 50 | |
| | M | 112 | |
| | W | 30 | |
| Blank thickness | | 1.6 | Steel |
| | | 2.5 | Aluminum |
| Die and punch radii | | 4 | |
| Clearance | | 0.9 | Steel |
| | | 1.0 | Aluminum |

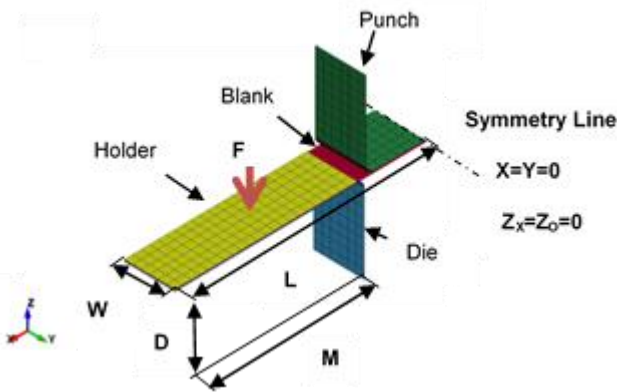


Figure 3: Theoretical model of U-drawing process, the 3D shell element

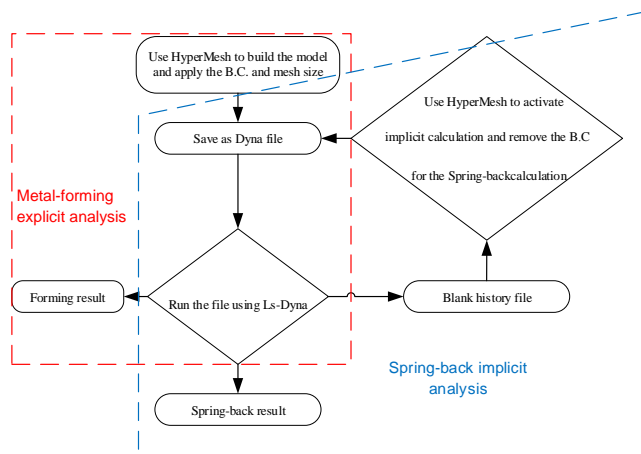


Figure 4: Flow chart for the numerical analysis of the U-drawing process and subsequent Spring-back (B.C. here)

denotes boundary conditions

Table 3: Yoshida-Uemori model, Young's modulus parameters and friction coefficients assumed for the four different materials [9]

| Parameters | DP600 | DX54D | CPLA10 0K38 | CPLA10 414 | |
|------------------------|---------|-------|-------------|------------|------|
| Y (MPa) | 326 | 145 | 150 | 60 | |
| B (MPa) | 143 | 30 | 75 | 60 | |
| c | 400 | 650 | 650 | 1500 | |
| b (MPa) | 120 | 60 | 10 | 30 | |
| m | 17 | 9 | 15 | 15 | |
| R _{sat} (MPa) | 188 | 170 | 95 | 150 | |
| h | 0.3 | 0.5 | 0.5 | 0.1 | |
| E _o [GPa] | 220.3 | 213.3 | 74 | 75.4 | |
| E _a [GPa] | 157 | 170 | 63 | 66 | |
| γ | 60 | 90 | 60 | 40 | |
| Friction coefficient | static | 0.31 | 0.29 | 0.37 | 0.27 |
| | dynamic | 0.25 | 0.26 | 0.34 | 0.27 |

The blank was segmented into five regions: I, II, III, IV and V with different meshing as shown in Figure 5. Each region has different mesh size to increase the accuracy of simulation analysis as well as minimising the simulation time. The mesh size was uniform and minimum in regions II to IV. However, the mesh size was linearly increased up to each free end using a 1.5 biasing ratio in regions I and V. Subsequently, the suitable mesh size in regions II to IV was 0.5 mm in the x-direction, where the results converged, therefore it was then used for all subsequent simulations.

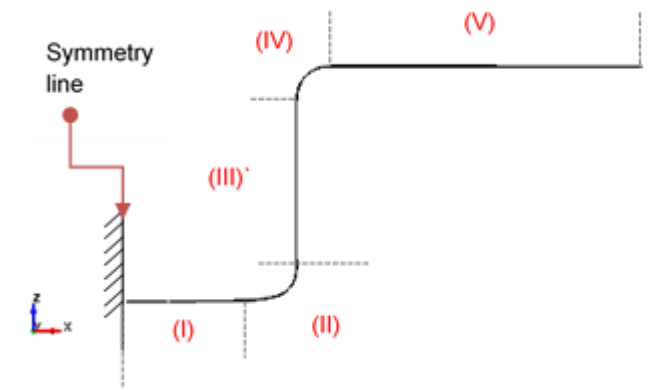


Figure 5: A mid-plane cross section for the U-deformed part

The Spring-back level was measured in this study by calculating the two angles θ_1 and θ_2 after U-drawing as mentioned in Figure 2 (b). Comparison between the numerical analysis of the Spring-back after U-drawing and experimental results was conducted for each blank material as listed in Table 4. It shows a general good agreement for all blank materials except the DP600 material where, there was a remarkable difference in θ_2 angle between numerical and experimental results. The reason of such disagreement is thought to be the presence of zinc coating on the surface of the DP600 which was not accounted in the numerical modelling. Although of such disagreement, the general

agreement between experiments and simulations for the rest blank materials ensures the validation of the numerical model. This led to use the same model for the following investigations such as parametric and optimisation studies.

Table 4: Experimental and 3D numerical simulation of Spring-back results for the four blank materials

| Material | Spring-back Angle (degrees) | | | |
|------------|-----------------------------|------------|------------|------------|
| | Experiment (average) | | Simulation | |
| | θ_1 | θ_2 | θ_1 | θ_2 |
| DP600 | 88.0 | 98.2 | 88.8 | 95.7 |
| DX54D | 88.5 | 91.7 | 87.9 | 92.1 |
| CPLA100k38 | 88.4 | 93.5 | 88.1 | 93.9 |
| CPLA 10414 | 88.4 | 91.5 | 88.9 | 92.1 |

Parametric study

The most important parameters of the U-drawing process namely the blank thickness, die radius and punch radius were considered. The validated 3D shell element model was utilised for all investigations. All parameters were kept constant as listed in Table 1 except one at a time was changeable.

The influence of the blank thickness.

The numerical simulations were repeated for different blank thicknesses in the range from 1 mm to 2.5 mm for all 4 materials. Figure 7 shows that the Spring-back magnitude varies along with the variation of blank thickness for all selected materials. Figure 7 (a) shows an increase in the angle θ_1 with the raise of blank thickness for tested materials which indicates a reduction in the level of Spring-back. Moreover, the Spring-back increases greatly for the bank of high strength material than the lower one. For example, the rate of Spring-back increase in DP600 is much greater than in DX54D. Furthermore, Figure 7 (b) illustrates that the Spring-back characterised by θ_2 angle decreases along with the increase of the blank thickness for all selected materials. Overall, both angles θ_1 and θ_2 represent the level of Spring-back occurring after the forming process which is clear in Figure 7 that the Spring-back level could be reduced by increasing the blank thickness. The same conclusion has been observed by other researchers [15]. Conversely, as the thickness is reduced (as is the case in many light-weight applications), the level of the Spring-back increases especially for the high strength DP600 steel which is why Spring-back is such an important issue for thin high strength blank materials.

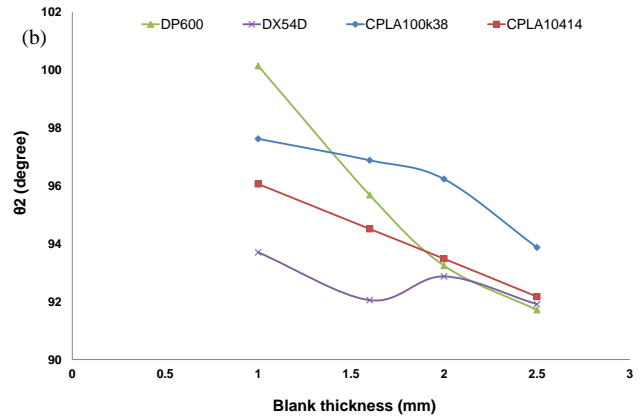
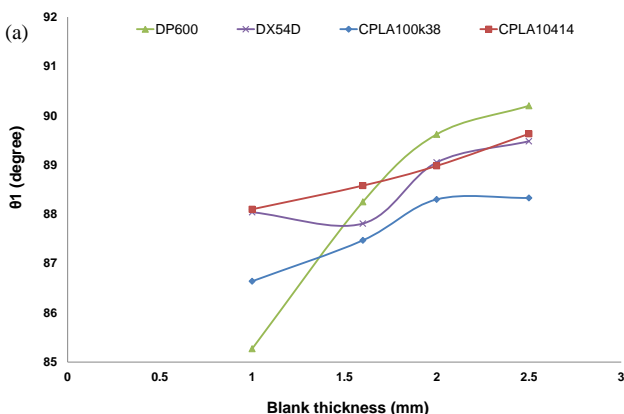


Figure 6: Predicted Spring-back after U-drawing for different blank thickness (a) θ_1 and (b) θ_2

The influence of the die radius.

In the current study 5 die radii were chosen to evaluate their effect on the level of Spring-back and they were varied from 4 to 12 mm in 2 mm intervals for all examined materials using the 3D validated model as mentioned earlier. Figure 8 explores the change in Spring-back magnitude, which is recognised again by both angles θ_1 and θ_2 , due to the variation of the die radius for all materials. Figure 8(a) shows slight increase for the angle of θ_1 towards the target angle (90°) with rise of the die radius which denotes in a reduction of the Spring-back. On the other hand Figure 8(b) shows a remarkable rise of the angle of θ_2 above 90° when the die radius between 4 and 6 mm and then increases gradually up to 12 mm of the die radius except the low strength steel material where the θ_2 angles remains almost the same.

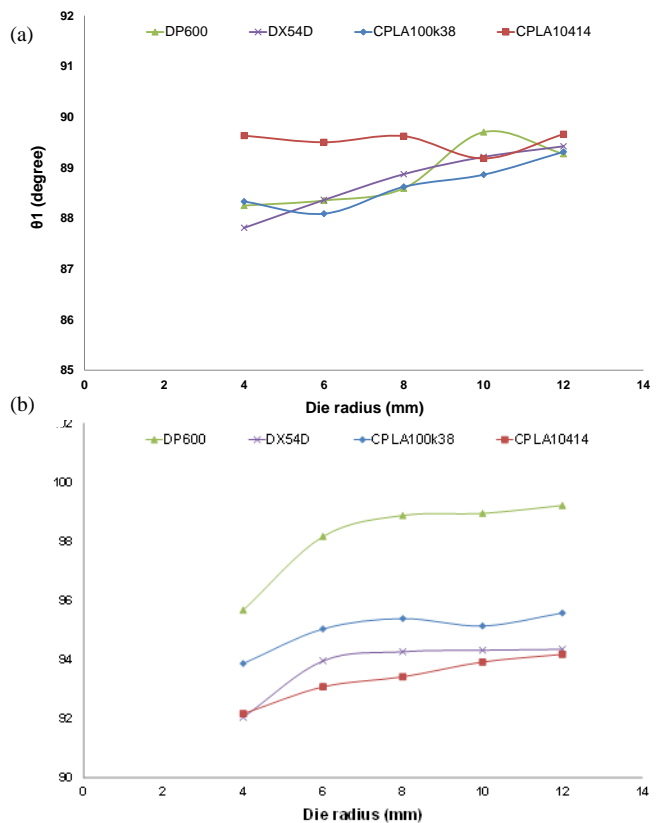


Figure 7: Predicted Spring-back after U-drawing for different die radii (a) θ_1 and (b) θ_2

For further understanding to the variation of Spring-back caused by changing in the die radius; principal total strains on both upper and lower surfaces were plotted for the high strength steel DP600 as shown in Figure 8, for the selected die radii. It can be observed that, the largest strains were located in both zones II and IV, where it is obvious from Figure 5 that these regions are related to the contact area around both punch radius and the die radius respectively. On the other hand, zone III explores a relatively smallest principal total strains with little variation which is represented the cross section area of the wall side as could be seen in Figure 5. Furthermore, an almost steady for the principal strain in region II were considered for the all three simulations because constant punch radius. However, the highest values of principal total strain in zone IV, along with the shortest deformed blank distance, were found for the lowest die radius and vice versa. This a good explanation about the reason of Spring-back reduction (angle θ_2) which was predicted for the low die radius as shown in Figure 7 (b).

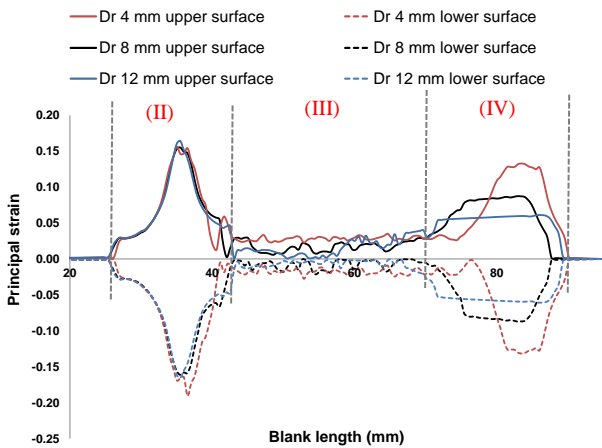


Figure 8: Maximum principal strain on upper and lower surface, for three different die radii for DP600 blank

The influence of the punch radius.

The punch radius used in the current study was started from 4 mm to 12 mm with interval of 2 mm for the four blank materials and other parameters were kept constant.

Figure 9 (a) shows a slight increase in θ_1 for all tested materials except for the low strength aluminium alloy shows almost steady behaviour along with punch radius change. This contributes to a little reduction in Spring-back level in these materials as the punch radius increases. However, the angle θ_2 was generally increased with the rise of the punch radius which implies an increase in the Spring-back level for all used material especially for the high strength one where the rate of increase was more pronounced for these materials than for the low strength one. The results shows that the θ_2 angle is more representative to the magnitude of the Spring-back therefore it is more considered in the current discussion.

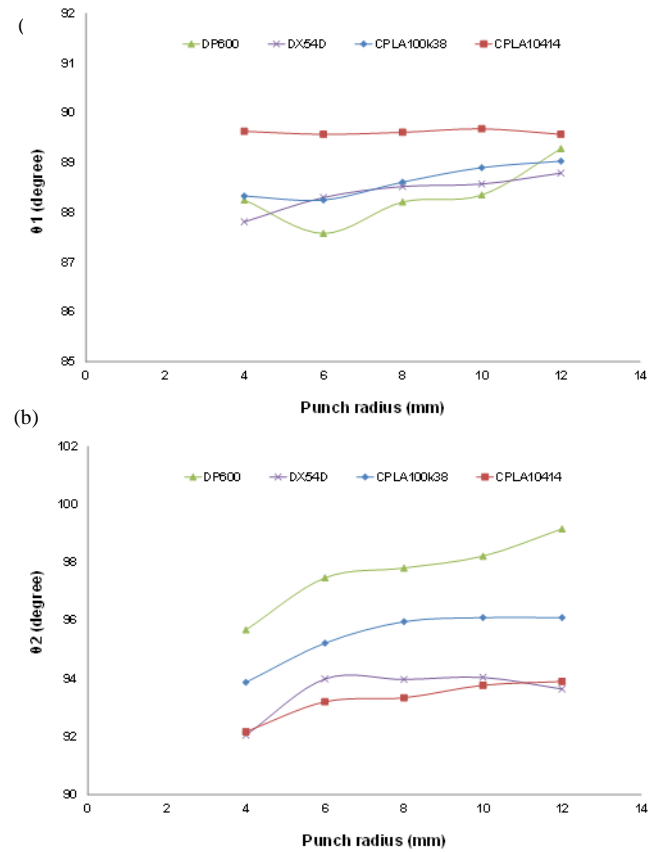


Figure 9: Predicted Spring-back after U-drawing for different punch radii (a) θ_1 and (b) θ_2

Similarly, the principal strain on both upper and lower surfaces of the DP600 steel were plotted for three different punch radii as shown in Figure 10. Obviously, the variation of the punch has main influence on the principal strain in (II) due to its close location as shown in Figure 10. However, it shows also a remarkable effect on the principal strain occur in (IV) which is close to the curvature of the die radius, although the die radius was kept constant at 4 mm for the three simulations. Figure 10 shows generally that the highest the highest principal strain in region II and IV was gained for the lowest punch radius of 4 mm. However, the lowest principal strain value was found when 12 and 8 mm of punch radius was modelled respectively. It was also observed that the more punch radius the wider distribution of principal strain in region (II). This led to better understanding about the reason of the punch radius influence on Spring-back level after the U-bending process. From both Figures (9 (b) and 10) it is clear that the more principal strain (which more plasticity in the blank materials), the lower Spring-back degree as shows in Figure 9 (b) where the minimum of the θ_2 angle was found when punch radius of 4 mm is used.

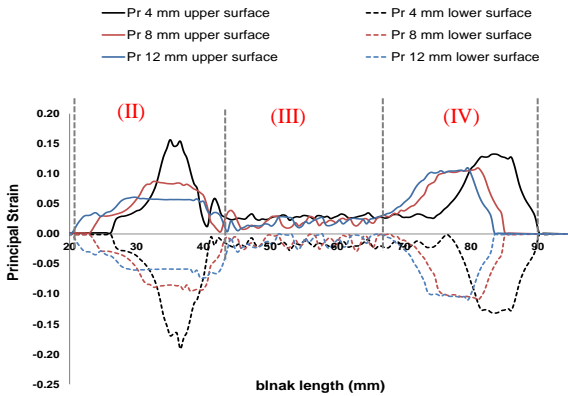


Figure 10: Maximum principal strain on upper and lower surface, for three different punch radii for DP600 blank

Optimisation

Parameters such as die radius, blank thickness, and punch radius were utilised for optimization study due to their remarkable effect on the Spring-back level. On the other hand, researchers were found that the clearance between the die and punch has insignificant effect [16].

In the current study the die and punch radii were varied while the blank thickness was kept constant. The optimization technique was utilised for the DP600 blank due to its sensitivity to the Spring-back phenomenon. The blank specification was the same one used in experiment with 1.6 mm thickness. Figure 11 outlines a developed generic optimisation technique. First, a Design of Experiments (DoE) was processed using the Optimal Latin Hypercube technique (OLH), as described in (Park, 1994) [17], to generate 30 combinations of the two design variables (die and punch radii). This technique drives uniform distributed points through a design space as shown in Figure 12. Two models were identify the DoE; the first was a building model and another was a validation model. The aim of each one is to increase the uniformity of the points within the space design.

The permutation genetic algorithm (Perm GA) described in (Narayanan et al., 2007) [18] was utilised using the OLH to produce uniform building and validation points. The Perm GA algorithm is conducted as follows: the design space has points with units of mass and these points apply gravity forces to each other; the potential energy of the system is then minimised. Subsequently, distribution of building and validation points were obtained, uniformly and not overlap as shown in Figure 12.

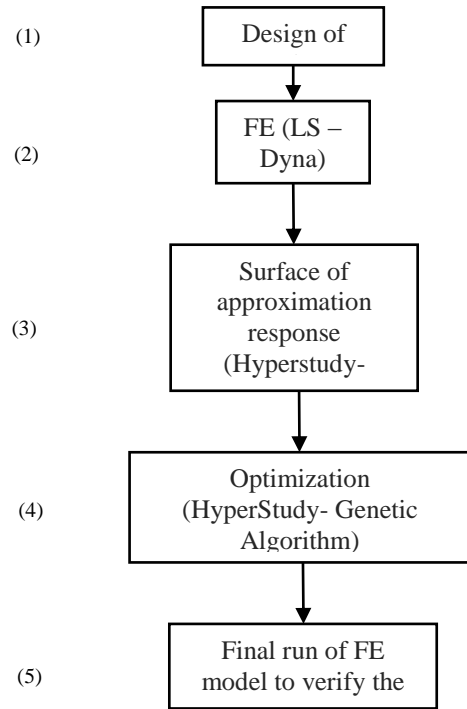


Figure 11: steps of optimisation techniques

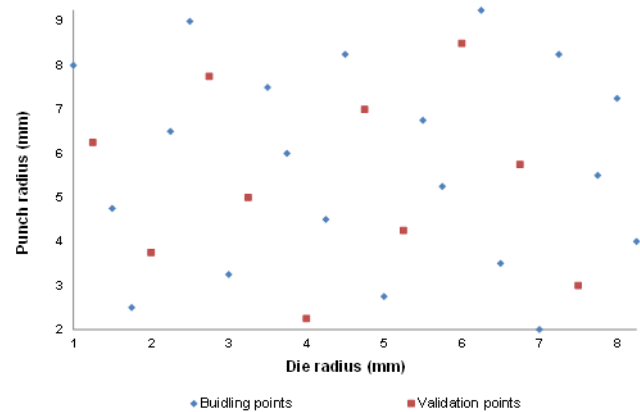


Figure 12: Building and validation points

Consequently, the validated 3-D shell finite element model was conducted for the DP600 high strength steel to calculate the Spring-back for the 30 designated points. Subsequently, an approximate response surface was plotted for the Spring-back within the design space using a Moving Least Squares (MLS) utilised in HyperStudy version 12 [19].

Figure 13 shows the variation of both angles, θ_1 and θ_2 which characterised the Spring-back after releasing the tools of the U-bending process within the design space. In Figure 13, the Z-direction denotes the angle magnitude, Y-direction and X – direction denote punch and die radii respectively. Figure 13 (b) shows a significant variation in θ_2 angle within the design space, however θ_1 angle has minor altering through the design space as shown in Figure 13 (a). Therefore, the current study has performed an objective function that most influences the Spring-back behaviour which is the angle θ_2 . Therefore, the genetic algorithm (GA) optimisation technique attainable

from Hyperstudy v12 of the Altair HyperWorks package was utilised. The main objective function was to minimise the angle θ_2 with the following constraints:

$$90 \leq \theta_2 \leq 92 \text{ (degree)}$$

$$88 \leq \theta_1 \leq 90 \text{ (degree)}$$

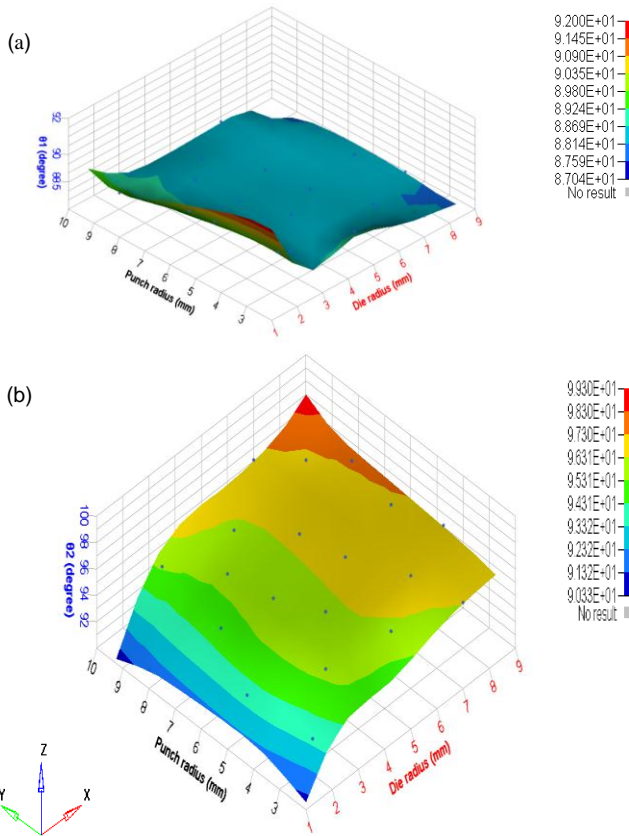


Figure 13: Response surface showing predicted Spring-back angle for the DP600 blank (a) θ_1 and (b) θ_2

The GA technique generated the optimum design variables to reduce the angle θ_2 as listed in Table 5 by build a model with die radius of 1 mm and punch radius of 8.25 mm. By utilising the optimisation approach the optimum angle values for both θ_1 and θ_2 were 89.34 and 91.41 degree respectively.

Table 5: Optimum and simulation results of the Spring-back after U-drawing for the DP600 blank for the two design variables

| Design variables | | Optimisation prediction | | Verification result | | Error | |
|------------------|-------------------|-------------------------|------------|---------------------|------------|------------|------------|
| Die radius (mm) | Punch radius (mm) | θ_1 | θ_2 | θ_1 | θ_2 | θ_1 | θ_2 |
| | | (degrees) | | | | | |
| 1 | 8.25 | 89.34 | 91.41 | 89.37 | 91.52 | 0.03 | 0.11 |

After that, the optimum design variable was utilised in the same model to verify the results of the optimisation. The results shows a very good agreement between both results which give more reliability on the optimisation technique used in the current study. Figure 14 shows the difference of the level of Spring-back between the initial design (when die and

punch radii were 4 mm) and the optimum one, where the punch radius was 8.25 mm and the die radius was 1 mm. There is a remarkable reduction of Spring-back for the optimum design comparing with the initial one. Although, the parametric study proves that the smaller the die or punch radii the less Spring-back. However when optimisation method utilised, the best combination of both punch and die radii that results in minimum level of elastic recover was when the die radius was minimum as 1mm and the punch at maximum level of 8.25 mm. This shows the robust and reliability of the optimisation method used in the current study which led to eliminate of the level of the elastic recover after the U-drawing process.

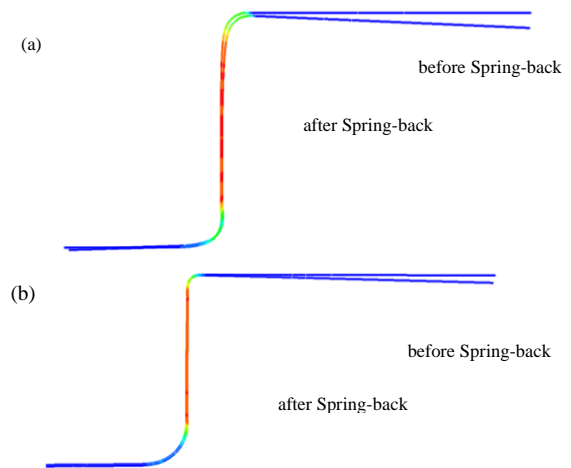


Figure 14: Final stage of U-drawing and the subsequent Spring-back for the DP600 blank for (a) the initial design (b) the optimum design

Similar to previous discussion, the distribution of principal strain at different regions (illustrated in Figure 5) of the DP600 blank material for the initial and optimum design were gained as shown in Figure 15. It was observed that optimum design led to more values in principal strain than the initial one which means that the DP600 blank steel that undergoes the U-drawing process with the optimum parameter, exposes to more plastic deformation than the initial one. That is clear in both regions (III) and (IV), where the principal strains are generally highest for the optimum design as shown in Figure 15.

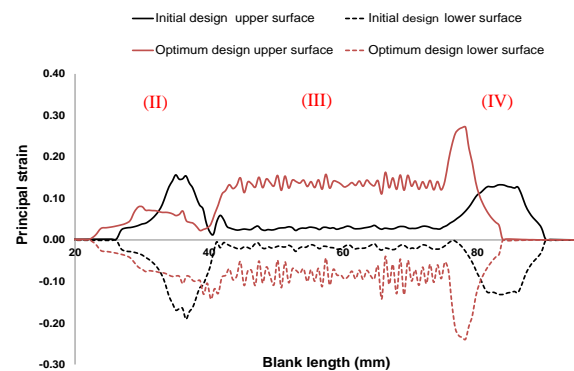


Figure 15: Maximum principal strain on upper and lower surfaces for initial and optimum designs for DP600 blank

Finally, the Ls-dyna was utilised to ensure the power of the optimisation technique to eliminate the level of Spring-back after the U drawing process. Therefore, in the current study, the U-drawing process for DP600 blank material was used as a case to observe the robust of the advanced CAD simultaneously with the optimisation technique, by running the Ls dyna using the same optimum design variables. As a result, a remarkable reduction in the level of Spring-back observed for the DP600 material when the optimum design variables were used as shown in Figure 15. Furthermore, the same optimum design variables were utilised also for the simulation of other blank materials and almost led to very lower level of Spring-back for the DX54D steel of 1.6 mm thicknesses as illustrated in Table 6. Conversely, these optimum design variables were not found suitable for the aluminium blank materials because that blank elements began to severe fold and distort at the region that moves over the die radius. It is obvious that optimum die radius (made of hard material) was less than the aluminium blank thickness (soft material). Subsequently, to overwhelm this concern, the size of element especially at critical area (II to IV) was minimise from 0.5 to 0.2 mm but unfortunately the same performance was detected, despite the huge consuming time. As a result, the suitable die radius was 2.5 mm and the punch radius was kept to be the same as the optimum value. After that, the simulation worked and a reduction in the level of Spring-back was obtained for the aluminium blank materials mentioned in Table 6.

Table 6: Spring-back predictions after U-drawing for all blanks for the initial and optimised designs.

| Material | Optimum design variables | | Initial design | | Optimum design | |
|------------|--------------------------|-------------------|----------------|------------|----------------|------------|
| | Die radius (mm) | Punch radius (mm) | θ_1 | θ_2 | θ_1 | θ_2 |
| | | | (degrees) | | | |
| DP600 | 1 | 8.25 | 88.78 | 95.68 | 89.37 | 91.52 |
| DX54D | 1 | 8.25 | 87.89 | 92.05 | 89.12 | 91.05 |
| CPLA100k38 | 2.5 | 8.25 | 88.07 | 93.87 | 89.33 | 91.91 |
| CPLA10414 | 2.5 | 8.25 | 88.85 | 92.07 | 89.90 | 91.95 |

CONCLUSION

The main objective of this research is to assess the power of the use of advanced computer aided design that utilised to predict Spring-back followed by most of the metal forming process. 3D shell element, the Yoshida-Uemori material model (considering the Bauschinger effect and the reduction in Young's modulus following plastic deformation), and the explicit and implicit analysis were utilised for forming and Spring-back analysis respectively as these together led to more acceptable and accurate results. Although there were good validation for all material used in this study, there was disagreement between numerical predictions and experiment for the coated high strength steel. This reveals the vital of modelling the effect of the coating in future studies.

A unique optimisation technique has been developed to eliminate Spring-back followed by the U-drawing process by optimising affected parameters. This scheme has been demonstrated to lead substantial decrease in Spring-back for all used materials. The application and verification of these advanced CAE techniques represent an important contribution to the study of sheet metal forming processes.

REFERENCES

- [1] JAGUAR LAND ROVER. Jaguar Land Rover Sustainability Report. Available Online: http://www.jaguar.co.uk/Images/Jaguar%20Land%20over%20Sustainability%20Report_Interactive_tcm91-69340.pdf [Accessed 01/12/2014], 2013.
- [2] MOHAMAD, J. B. Spring-backprediction in sheet metal forming: constitutive equations, finite element simulations and experimental validation. PhD Thesis, University of Strathclyde, 2013.
- [3] EGGERTSEN, P. A. & MATTIASSON, K. On the modelling of the bending-unbending behaviour for accurate Spring-backpredictions. International Journal of Mechanical Sciences, 51, 547-563, 2009.
- [4] EGGERTSEN, P. A. & MATTIASSON, K. On constitutive modeling for Spring-backanalysis. International Journal of Mechanical Sciences, 52, 804-818, 2010.
- [5] HASEGAWA, T., YAKOU, T. & KARASHIMA, S. Deformation behaviour and dislocation structures upon stress reversal in polycrystalline aluminium. Materials Science and Engineering, 20, 267-276, 1975.
- [6] CHRISTODOULOU, N., WOO, O. T. & MACEWEN, S. R. Effect of stress reversals on the work hardening behaviour of polycrystalline copper. Acta Metallurgica, 34, 1553-1562, 1986.
- [7] WILSON, D. V. & BATE, P. S. Reversibility in the work hardening of spheroidised steels. Acta Metallurgica, 34, 1107-1120, 1986.
- [8] YOSHIDA, F. & UEMORI, T. A model of large-strain cyclic plasticity describing the Bauschinger effect and workhardening stagnation. International Journal of Plasticity, 18, 661-686, 2002.
- [9] ALGHTANI.A.H. Analysis and Optimization of springback in sheet metal forming . University of Leeds, 2015.
- [10] BENSON, D. J., BAZILEVS, Y., HSU, M. C. & HUGHES, T. J. R. Isogeometric shell analysis: The Reissner–Mindlin shell. Computer Methods in Applied Mechanics and Engineering, 199, 276-289, 2010.
- [11] BISCHOFF, M., BLETZINGER, K. U., WALL, W. A. & RAMM, E. Models and Finite Elements for Thin-Walled Structures. Encyclopedia of Computational Mechanics. John Wiley & Sons, Ltd, 2004.
- [12] LEE, S. W. & YANG, D. Y. An assessment of numerical parameters influencing Spring-backin explicit finite element analysis of sheet metal forming process. Journal of Materials Processing Technology, 80–81, 60-67, 1998.
- [13] NARASIMHAN, N. & LOVELL, M. Predicting Spring-backin sheet metal forming: an explicit to

- implicit sequential solution procedure. Finite Elements in Analysis and Design, 33, 29-42, 1999.
- [14] BEHROUZI, A., DARIANI, B. M. & SHAKERI, M. A new approach for inverse analysis of Spring-back in a sheet-bending process. Proceedings of the Institution of Mechanical Engineers, Part B: Journal of Engineering Manufacture, 222, 1363-1374, 2008.
- [15] RAHMANI, B., ALINEJAD, G., BAKHSHI-JOOYBARI, M. & GORJI, A. An investigation on springback/negative Spring-back phenomena using finite element method and experimental approach. Proceedings of the Institution of Mechanical Engineers, Part B: Journal of Engineering Manufacture, 223, 841-850, 2009.
- [16] LAJARIN, S. F. & MARCONDES, P. V. Influence of process and tool parameters on Spring-back of high-strength steels. Proceedings of the Institution of Mechanical Engineers, Part B: Journal of Engineering Manufacture, 229, 295-305, 2015.
- [17] PARK, J.-S. Optimal Latin-hypercube designs for computer experiments. Journal of Statistical Planning and Inference, 39, 95-111, 1994.
- [18] NARAYANAN, A., TOROPOV, V. V., WOOD, A. S. & CAMPEAN, I. F. Simultaneous model building and validation with uniform designs of experiments. Engineering Optimization, 39, 497-512, 2007.
- [19] HYPERSTUDY, V. 12 ed.: Altair Engineering, 2012.